ASSESSING AGRICULTURAL BURNED AREAS USING dNBR INDEX FROM SENTINEL-2 SATELLITE DATA IN CHIANG MAI, THAILAND, FROM 2019 TO 2023

Ratchaphon SAMPHUTTHANONT [1,2]

DOI: 10.21163/GT_ 2024.192.04

ABSTRACT

This study conducted an assessment of agricultural burned areas using the dNBR index from Sentinel-2 satellite data, HARMONIZED collection, in Mae Rim District, Chiang Mai Province, over 5 years from 2019 to 2023. A total of 118 satellite datasets, before and after burning, were used to analyze the severity levels. It is considered severe once the Moderate Low Severity level is above 0.27. Error correction employed scene classification data, derived from the European Space Agency's area classification algorithms, and the NDWI index was used to exclude water-covered areas. Accuracy verification through an Error Matrix was conducted at 73 survey points with a 95% confidence level, adhering to the principles of statistical probability. The overall accuracy of the burned area classification was 82.19%. Agricultural burned areas in the study area were predominantly found mostly on flat terrain. in the eastern direction. In general, there was a significant increasing trend in burning, especially in the latest year 2023. Changes in the distribution burning month distribution were observed; in 2019-2022 burning was more prevalent in May, while in 2023, it shifted to April. This study successfully detected rice field burning; a small-scale, low fuel load, and low temperature burning, which the satellite hotspot data could not detect such burning. The results provide valuable information to promote the creative reduction of burning in communities by utilizing post-harvest agricultural residue, demonstrating the timely and appropriate application of tools and data for societal benefits.

Keywords: *Agricultural Burned Area, Remote Sensing, Difference Normalized Burn Ratio (dNBR), Sentinel-2*

1. INTRODUCTION

Chiang Mai province, located in the northern region of Thailand, faces air pollution issues, particularly due to high levels of fine particulate matter (PM2.5), which exceed standards for many months especially during the dry season from the end of a year to the middle of another year (Buakhao, 2023). Open biomass burning (OBB), which typically involves in-field agricultural residues, is a significant source of air pollution. It releases various pollutants and particulate matter, including Total Particulate Matter (TPM), in significant quantities (Rongmuang, 2015).

Currently, remote sensing data are being utilized for monitoring, tracking, and assessing open burning areas. Various satellite data sources such as MODIS and Landsat are used for this purpose, whereas the popularity of Sentinel-2 satellite data has grown due to its superior spatial resolution capabilities, providing higher definition than other satellites (Linta et al., 2021). The Normalized Burn Ratio (NBR) is commonly used to classify and assess the severity of burned areas (García, 1991; Alcaras, 2022), proving high efficiency in identifying vegetation affected by fire (Boulghobra, 2021; Kovacs, 2019; Mohammad, 2023). It is the ratio between Near Infrared (NIR) and Short-Wave Infrared (SWIR)

[1] *Department of Geography and Geoinformatics, Faculty of Humanities and Social Sciences, Chiang Mai Rajabhat University, Thailand, ratchaphon_sam@cmru.ac.th*

[2] *Asian Air Quality Operations Center by Space Technology, Geoinformatics & Environmental Engineering (AiroTEC), Chiang Mai Rajabhat University, Thailand*

bands used by Alcaras (2022). However, assessing such burned areas using this method may introduce errors when overlapping with water bodies, built-up areas, and other land covers, which are considered as the least likelihood of burning (Khamrueangwong, 2021).

This study focused on classifying agricultural burned areas using Sentinel-2 satellite data in the Mae Rim District, Chiang Mai Province, from 2019 to 2023. The main emphasis was on post-harvest rice field areas, which are frequently subjected to burning, to analyze spatial and temporal changes in burned areas. The analysis involved filtering out non-vegetation-covered areas using Sentinel-2 Scene Classification data and classifying burned areas using the Difference Normalized Burn Ratio (dNBR) method. To enhance the accuracy of burned area classification., water-covered areas were excluded from the results. Additionally, field surveys were conducted to verify accuracy and facilitate activities in order to provide alternative solutions for farmers to utilize post-harvest agricultural residues, thereby reducing burning. The study area, located in the Mae Rim district of Chiang Mai province, comprises a significant portion of rice fields. To promote reduction of agricultural burning, farmers and various agencies are coordinated to integrate knowledge for public benefits.

2. STUDY AREA

The study area is the Mae Rim District, Chiang Mai province (**Fig. 1**). Data on land use within the Mae Rim district in 2021 were classified by the Department of Land Development using visual interpretation in combination with aerial photography and satellite imagery. It revealed a total agricultural area of 76,131.53 rai, accounting for 26.56% of the study area.

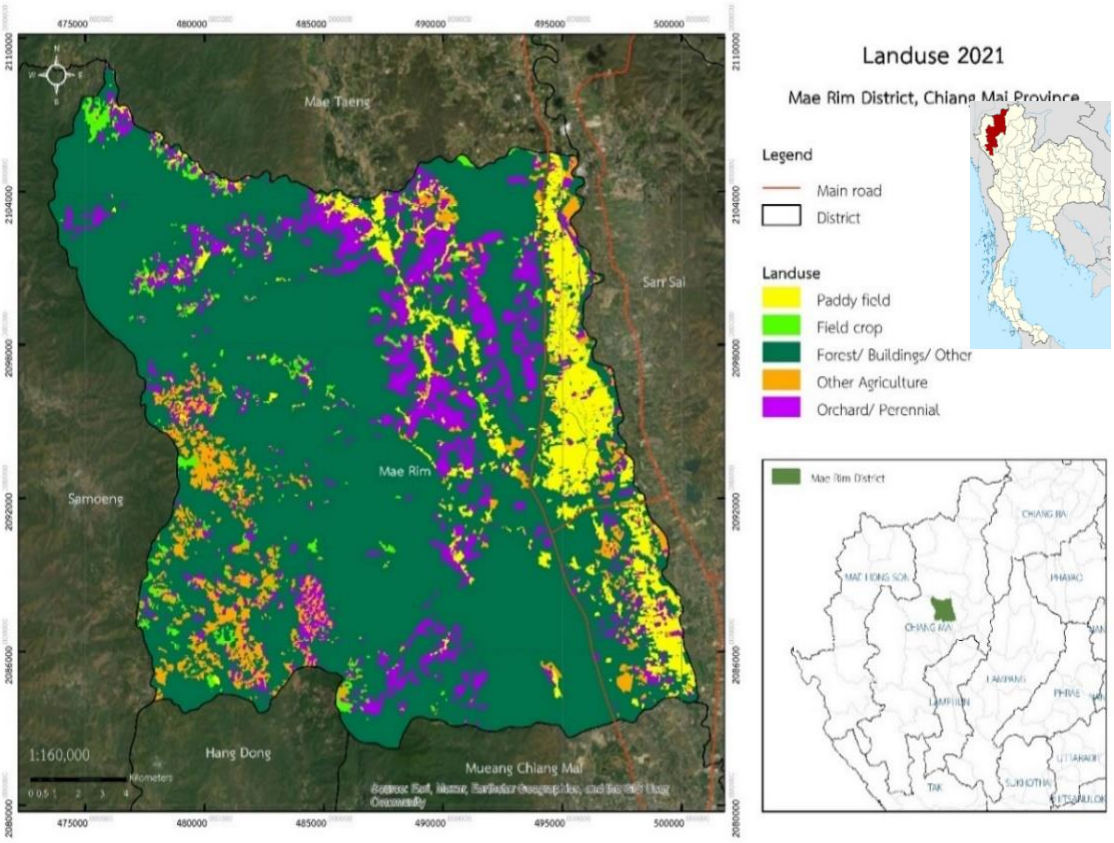

Fig. 1. Study Area and Land Use, Mae Rim District, Chiang Mai Province.

The predominant land use was rice cultivation where rice straw and stubble burning is a common practice among farmers. This burning significantly contributes to air pollution, causing health problems and soil fertility degradation.

3. DATA AND METHODS

3.1. Data Preparation from Satellite

Data preparation was carried out using Sentinel-2 satellite data from the HARMONIZED collection under the Harmonized Landsat and Sentinel-2 program by NASA. The objective was to generate a dataset that reflects surface reflectance jointly captured by the Operational Land Imager (OLI) on Landsat-8/9 satellites and the Multi-Spectral Instrument (MSI) on Sentinel-2A/B satellites (NASA, 2023). Due to ESA's adjustment of the processing baseline on January 26, 2022, digital number (DN) limitations were introduced in the original data, allowing negative values which were not possible previously. Therefore, to analyze these changes as smoothly as possible, the Sentinel-2 HARMONIZED collection dataset (Sentinelhub, 2021) was used to analyze burned areas within agricultural land post-harvest. Analysis involved assessing the difference in Normalized Burn Ratio (NBR) values between pre- and post-burning periods from January to May and November to December, excluding periods with heavy cloud cover during the rainy season where soil cover data could not be accurately recorded. Thus, satellite data before and after burning within a 5-year period from 2019 to 2023 were selected for analysis, totalling 118 datasets as shown in **Table 1**.

3.2. Normalized Burn Ratio (NBR) Analysis

Analysis to assess burned areas using the Normalized Burn Ratio (NBR) index is designed to differentiate areas affected by large wildfires. Evergreen areas reflect strongly in the Near Infrared (NIR) wavelength range and has low reflectance in the Short-Wave Infrared (SWIR) range, which is opposite to what is observed in the burning areas. Therefore, burned areas can be distinguished by the difference in NBR values between pre- and post-burning periods (Keeley, 2009), as illustrated in Equation 1 (García, 1991; Alcaras, 2022).

$$NBR = (NIR - SWIR)/(NIR + SWIR) \quad (1)$$

For Sentinel-2 satellite data, Equation 2 (Al-hasn et al., 2022)

$$NBR_{Sentinel-2} = \frac{(Band\ 8 - Band\ 12)}{(Band\ 8 + Band\ 12)} \quad (2)$$

3.3. Analysis of Differences in NBR between Pre- and Post-Burning Periods

To analyze the burned areas, the differences in the Normalized Burn Ratio (NBR) index must be assessed. This is achieved by calculating the difference in the Different Normalized Burn Ratio (dNBR) between the pre-burning and post-burning periods (Kovacs, 2019), as shown in Equation 3.

$$d\ NBR = (NBR_{Pre-fire} - NBR_{Post-fire}) \quad (3)$$

Table 1.

Satellite Data for Pre- and Post-Burning Analysis for the Years 2019 – 2023.

2019			2020			2021			2022			2023		
no.	Pre-fire	Post-fire	no.	Pre-fire	Post-fire	no.	Pre-fire	Post-fire	no.	Pre-fire	Post-fire	no.	Pre-fire	Post-fire
1	18 Dec 2018	15 Jan	28	31 Dec 2019	10 Jan	47	25 Dec 2020	4 Jan	73	25 Dec 2021	9 Jan	94	20 Dec 2022	9 Jan
2	15 Jan	20 Jan	29	10 Jan	15 Jan	48	4 Jan	14 Jan	74	9 Jan	24 Jan	95	9 Jan	14 Jan
3	20 Jan	30 Jan	30	15 Jan	25 Jan	49	14 Jan	19 Jan	75	24 Jan	3 Feb	96	14 Jan	24 Jan
4	30 Jan	4 Feb	31	25 Jan	30 Jan	50	19 Jan	24 Jan	76	3 Feb	8 Feb	97	24 Jan	3 Feb
5	4 Feb	9 Feb	32	30 Jan	4 Feb	51	24 Jan	3 Feb	77	8 Feb	13 Feb	98	3 Feb	8 Feb
6	9 Feb	14 Feb	33	4 Feb	14 Feb	52	3 Feb	13 Feb	78	13 Feb	5 Mar	99	8 Feb	13 Feb
7	14 Feb	19 Feb	34	14 Feb	5 Mar	53	13 Feb	28 Feb	79	5 Mar	10 Mar	100	13 Feb	18 Feb
8	19 Feb	24 Feb	35	5 Mar	30 Mar	54	28 Feb	5 Mar	80	10 Mar	15 Mar	101	18 Feb	23 Feb
9	24 Feb	1 Mar	36	30 Mar	19 Apr	55	5 Mar	15 Mar	81	15 Mar	20 Mar	102	23 Feb	28 Feb
10	1 Mar	6 Mar	37	19 Apr	4 May	56	15 Mar	20 Mar	82	20 Mar	25 Mar	103	28 Feb	15 Mar
11	6 Mar	11 Mar	38	4 May	14 May	57	20 Mar	25 Mar	83	25 Mar	29 Apr	104	15 Mar	20 Mar
12	11 Mar	21 Mar	39	10 Nov	15 Nov	58	25 Mar	14 Apr	84	29 Apr	4 May	105	20 Mar	4 Apr
13	21 Mar	26 Mar	40	15 Nov	20 Nov	59	14 Apr	19 Apr	85	10 Oct	5 Nov	106	4 Apr	24 Apr
14	26 Mar	4 Apr	41	20 Nov	25 Nov	60	19 Apr	24 Apr	86	5 Nov	10 Nov	107	24 Apr	29 Apr
15	4 Apr	15 Apr	42	25 Nov	30 Nov	61	24 Apr	4 May	87	10 Nov	15 Nov	108	29 Apr	4 May
16	15 Apr	20 Apr	43	30 Nov	5 Dec	62	4 May	9 May	88	15 Nov	20 Nov	109	4 May	19 May
17	20 Apr	25 Apr	44	5 Dec	10 Dec	63	9 May	14 May	89	20 Nov	30 Nov	110	19May	24 May
18	25 Apr	30 Apr	45	10 Dec	15 Dec	64	14 May	29 May	90	30 Nov	5 Dec	111	10Nov	20 Nov
19	30 Apr	15 May	46	15 Dec	25 Dec	65	5 Nov	15 Nov	91	5 Dec	10 Dec	112	20Nov	25 Nov
20	15 May	20 May				66	15 Nov	20 Nov	92	10 Dec	15 Dec	113	25Nov	5 Dec
21	16 Nov	26 Nov				67	20 Nov	30 Nov	93	15 Dec	20 Dec	114	5 Dec	10 Dec
22	26 Nov	1 Dec				68	30 Nov	5 Dec				115	10 Dec	15 Dec
23	1 Dec	11 Dec				69	5 Dec	10 Dec				116	15 Dec	20 Dec
24	11 Dec	16 Dec				70	10 Dec	15 Dec				117	20 Dec	25 Dec
25	16 Dec	21 Dec				71	15 Dec	20 Dec				118	25 Dec	30 Dec
26	21 Dec	26 Dec				72	20 Dec	25 Dec						
27	26 Dec	31 Dec												

3.4. Classification of Burn Severity Levels

In this study, burned areas were classified based on the wildfire severity levels, which are into 7 levels by The United States Geological Survey (USGS). Among these, three levels indicate areas affected by fire are Moderate-low Severity, Moderate-high Severity, and High Severity. Specifically, the Moderate low Severity level is defined as having values higher than 0.27, indicating areas burned by wildfires.

3.5. Analysis of Post-Harvest Bare Areas

Areas covered by clouds, cloud shadows, and water bodies can introduce errors in the classification of burned areas. In this study, the results of the burned area classification overlapping with areas covered by vegetation, clouds, cloud shadows, and water bodies were removed. This was achieved using scene classification data, derived from the European Space Agency's (ESA) algorithm for land cover classification. The classification includes 12 different categories: No Data, Saturated or defective pixel, Topographic casted shadows, Cloud shadows, Vegetation, Not-vegetated, Water, Unclassified, Cloud medium probability, Cloud high probability, Thin cirrus, Snow or ice. Therefore, in this step, only post-harvest bare areas (Not-vegetated: Value = 5) were selected for analysis.

3.6. Analysis of Water-covered Areas

During the initial stages of rice cultivation, there is noticeable water coverage. To reduce errors in the classification of burned areas, Normalized Difference Water Index (NDWI) is used to monitor changes related to water quantity in water bodies. Since water bodies absorb light significantly in the electromagnetic spectrum, the visible spectrum (green) and the near-infrared spectrum are observed. Equation 4 illustrates this process. For Sentinel-2 data, Equation 5 is applied.

$$\text{NDWI} = (\text{green} - \text{near infrared}) / (\text{green} + \text{near infrared}) \tag{4}$$

$$NDWI_{Sentinel-2} = \frac{(Band\ 3 - Band\ 8)}{(Band\ 3 + Band\ 8)} \tag{5}$$

Then, water-covered areas are created by selecting only the NDWI areas with values greater than or equal to 0.25, which is determined by considering coverage of the initial stages of rice cultivation.

3.7. Verification of the accuracy of the burnt area classification.

Accuracy of the burnt area classification in this study was verified through random sampling points, with the sample size determined using the principle of binomial probability (Chucheep, 2018) as shown in Equation 6.

$$n = \frac{Z^2(p)(q)}{e^2} \tag{6}$$

where:

n = minimum sample size (number of sampling points)
p = probability of correctness (ranges from 0 to 1)
q = probability of error (ranges from 1 - p)
Z = value from the standard normal distribution table
e = margin of error from sampling

It was, then, distributed in the form of an Error Matrix or Contingency Table, which can be used to analyze the Producer's Accuracy, indicating the method's efficiency, the User's Accuracy, and the Overall Accuracy. (Chucheep, 2018) as shown in equations 7 - 9. The entire sequence of work steps is illustrated in **Fig. 2**.

$$\text{Producer's Accuracy} = \frac{n_{ii}}{n_{+j}} \tag{7}$$

$$\text{User's Accuracy} = \frac{n_{ii}}{n_{i+}} \tag{8}$$

$$\text{Overall Accuracy} = \frac{\sum_{i=1}^{k} n_{ii}}{n} \tag{9}$$

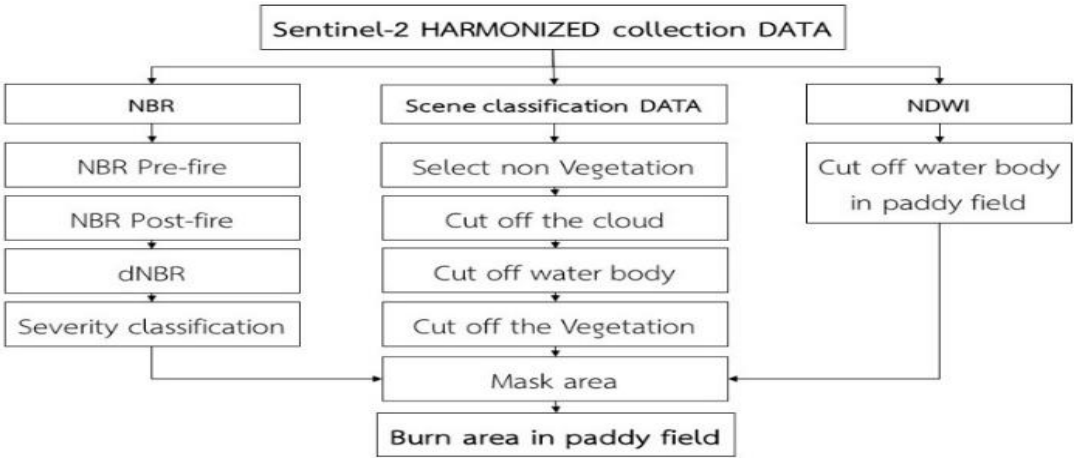

Fig. 2. The conceptual framework for analyzing burned areas in paddy fields using the dNBR index from Sentinel-2 satellite data.

4. RESULTS AND DISSUSSION

4.1. Fire Incidents and Trends in Agricultural Areas from 2019 to 2023

The changes in burned areas in rice fields in terms of both area and time revealed a higher incidence of burning during the months of April to May and November to December, corresponding to the post-harvest period (**Tab. 2**). Interestingly, during April to May 2023, there was a distinct shift in burning patterns, with more burning observed in April compared to May, which differs from the burning pattern during April to May of the years 2019-2022.

Table 2.

Displays the burned area in open fields (in hectares) categorized by month for the years 2019 to 2023.

Year/ Month	JAN	FEB	MAR	APR	MAY	NOV	DEC	sum
2019	2.18	3.19	6.61	45.63	239.81*	186.98	188.14	672.55
2020	1.21	0.7	4.48	30.78	167.14*	120.55	11.71	336.56
2021	6	2.06	12.14	28.92	127.67*	124.79	65.96	367.54
2022	2.54	33.01	28.52	11.74	558.29*	113.69	25.16	772.97
2023	40.15	34.21	39.08	715.03*	174.41	52.06	71.93	1126.87

** The month with the highest burning of the year.*

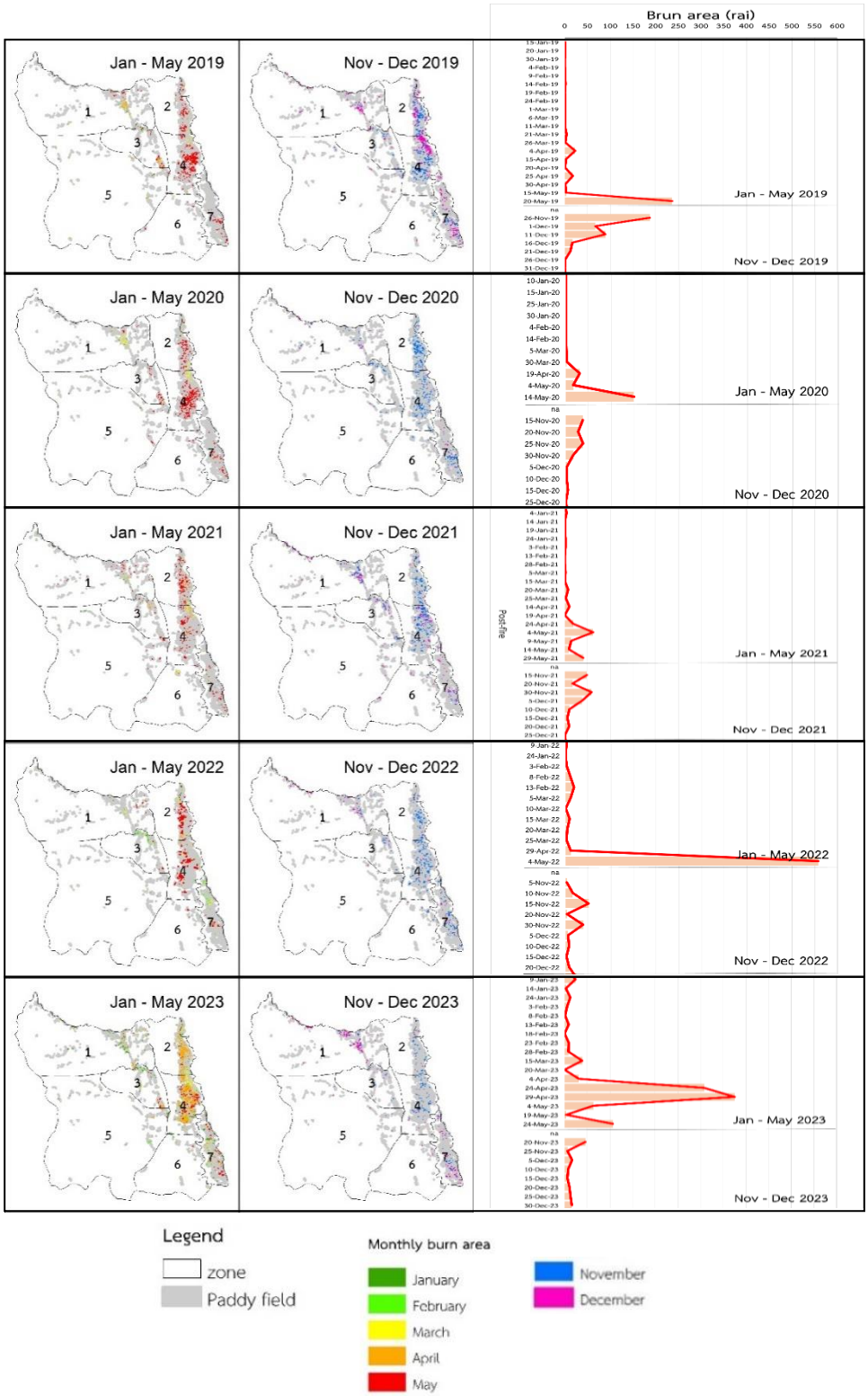

Fig. 3. Map of burned areas categorized by month from 2019 to 2023 (left), and line graph showing burned areas categorized by time intervals from 2019 to 2023 (right).

Due to the early onset of rain in April 2023 compared to previous years, farmers began burning stubble before planting as early as April. In contrast, from 2019 to 2022, the rainy season typically started in May, and the burning of stubble began accordingly. Meanwhile, it was observed that the burned areas tended to decrease from November to December during the years 2019-2023. Furthermore, each area exhibited somewhat consistent burning behavior, such as the upper part of Zone 4 burning faster than the lower part, as depicted in **Fig. 3.** In this study, the NDWI index was applied to extract burned areas in conjunction with other indices, enhancing efficiency, consistent with the study by Khamrueangwong (2021). For the date of the large fire event occurring on April 29, 2023, **Fig. 4** presents sample results of burn area, NBR, dNBR, NDWI, and scene classification.

Regarding the study on air pollution emissions resulting from burning in rice fields in Thailand, it was found that in 2018, burning covered 2.9% of the total rice cultivation area for that year (Junpen et al., 2018). This closely aligns with the burned areas observed in rice fields in Mae Rim District from 2019 to 2023, which accounted for 2.91%, 1.46%, 1.59%, 3.35%, and 4.88% respectively. However, a report in 2021 indicated that the northern region of Thailand had the highest incidence of burning in rice fields, accounting for 41.85% of the total rice cultivation area (Kanjanarueng, 2023).

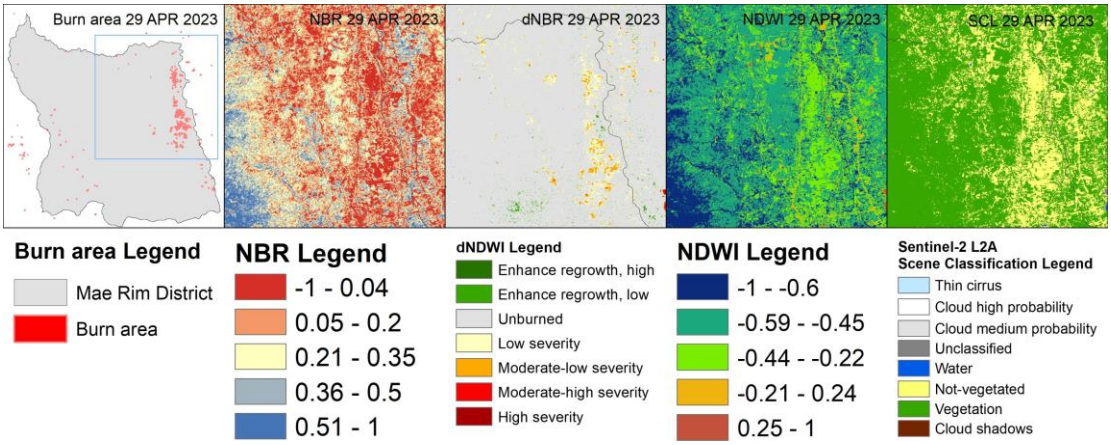

Fig. 4: Illustrates sample results of Burn area, NBR, dNBR, NDWI and Scene classification.

4.2. Verification of Burned Area Classification Accuracy

To verify accuracy of the burned area classification in this study, 73 sampling points were designated according to the criterion of binomial probability with a confidence level of 95%. These points were divided into 37 burned areas and 36 unburned areas. The results revealed that the classification of burned areas showed a producer's accuracy of 90% and a user's accuracy of 72.97%. Regarding the classification of unburned areas, the producer's accuracy was 76.74%, and the user's accuracy was 91.67%. The overall accuracy was found to be 82.19%, as shown in **Table 3** and **Fig. 5**.

Table 3.

Error Matrix of Fire Area Classification.

		Reference data from field			
		burn	**non-burn**	**SUM**	**User's Accuracy (%)**
Classified image	**burn**	**27**	10	37	72.97
	non-burn	3	**33**	36	91.67
	SUM	30	43	**73**	
	Producer's Accuracy (%)	90	76.74		

Overall Accuracy (%) = 82.19

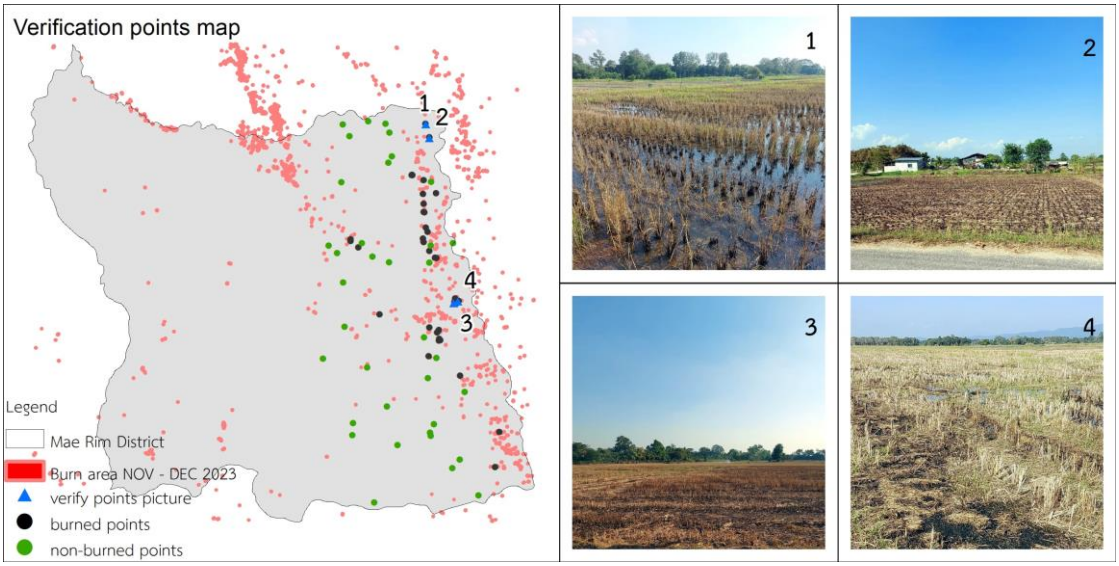

Fig. 5. Field Survey of Sample Areas.

In summary, the classification of burned areas in this study demonstrated a method efficiency of 90% and a reliability of 72.97%, while for unburned areas, it showed a method efficiency of 76.74% and a reliability of 91.67%. Overall, the classification accuracy in this study was 82.19% at a 95% confidence level. This validation method is commonly used for analyzing burned areas from satellite data. (Ruthamnong, 2019; Katagis, 2022).

4.3. Comparing Fire Detection between Hotspot Data and Satellite Imagery

Hotspot data refers to the Land Surface Temperature, especially abnormally high temperatures on the Earth's surface. The data can signify intense fire activity and even pinpoint the location of fire origins. At present, the Department of Forestry of Thailand utilizes the Visible Infrared Imaging Radiometer Suite (VIIRS) data onboard the Suomi National Polar-orbiting Partnership (Suomi-NPP) satellite which can capture global images every 12 hours, twice a day. The fire hotspot locations within a 375 x 375-meter area are accounted as a single data point. This data is considered before identifying areas with forest fire incidents and to monitor regions prone to frequent fire occurrences (Praesriwarothai, 2021).

When examining a composite image of Shortwave Infrared (SWIR) and True Color from Sentinel-2 satellite imagery, it becomes evident that areas of active burning and smoke plumes are clearly delineated.

Fig. 6. A composite of Shortwave Infrared (SWIR) and True Color imagery from Sentinel-2 satellite data during the occurrence of burning within rice field areas where hotspots could not be detected.

However, during the same timeframe, no hotspot data is available. This indicates that fire occurrences in rice fields, particularly smaller, low-intensity burns with lower burning temperatures, are better detected through dNBR index of satellite imagery compared to hotspot data, which may not be captured (GISGeography, 2024). This aligns with the findings of Mohammad (2023), which discovered that dNBR from Sentinel-2 outperforms in spectral discrimination between burned and unburned surfaces. This is illustrated in **Fig. 6**.

5. CONCLUSIONS

The area burned delineation in this study focused on categorizing burned areas within rice field areas after harvesting over a period of 5 years (2019 - 2023) using Sentinel-2 HARMONIZED satellite data, analyzed from the Normalized Burn Ratio (NBR) difference values before and after burning, with a threshold of Moderate Low Severity (0.27) and above indicating burned areas. Areas covered by dense vegetation, water bodies, and clouds/shadows were excluded using Sentinel-2 L2A Scene Classification and NDWI data. Accuracy of the classification was evaluated using an Error Matrix with 73 survey points at a 95% confidence level, following the principles of probabilistic sampling. The results showed that the burned area in rice fields was 672.55, 336.56, 367.54, 772.97, and 1,126.87 rai per year, respectively. It was observed that the burned area was higher during April to May and November to December, which corresponded to the post-harvest period within the study area. In April 2023, there was a significant increase of burned areas compared to other years. On the contary, it was found that during November to December of each year, the burned area tended to decrease. Furthermore, distinct patterns of burning before and after harvesting were observed in each area. Overall accuracy of the classification in this study was 82.19%. Regarding the burned area classification, there was a 72.97%.

ACKNOWLEDGEMENT

I would like to express my gratitude to UNDP, GIZ, and WHO for their support of the "Clean Air Without Border" project, a collaborative initiative between Thailand and Laos, aiming for innovatively addressing air pollution issues. Their support has enabled research and community-based activities to reduce burning creatively. Additionally, I extend my thanks to AiroTEC, CMRU for their invaluable assistance and facilitation, which greatly contributed to the success of the research endeavor.

REFERENCES

Alcaras, E., Costantino, D., Guastaferro, F., Parente, C., & Pepe, M. (2022). Normalized Burn Ratio Plus (NBR+): A New Index for Sentinel-2 Imagery. Remote Sensing, 14(7), 1727. https://doi.org/10.3390/rs14071727

Al-hasn R., & Almuhammad R. (2022). Burned area determination using Sentinel-2 satellite images and the impact of fire on the availability of soil nutrients in Syria. Journal of Forestry Science, 68(3), 96–106.

Boulghobra, N. (2021). Sentinel 2 Imagery and Burn Ratios for Assessing the July 5, 2021 Wildfires Severity in the Region of Khenchela (Northeast Algeria). Geographia Technica, 16 (2), 95-104. DOI: 10.21163/GT_2021.162.08

Buakhao, L. (2023). Model for Estimating PM2.5Concentration Using Aerosol Optical Depth Data in the Muang District of Chiang Mai Province. YRU Journal of Science and Technology, 8(1), 50-58.

Chucheep, K. (2018). Accuracy Assessment. Remote Sensing Technical. Note No. 3 (2018). Faculty of Forestry, Kasetsart University.

García, M.J.L., & Caselles, V. (1991). Mapping burns and natural reforestation using thematic mapper data. Geocarto International, 6(1), 31–37.

GIS Geography. (2024). Sentinel 2 Bands and Combinations. Retrieved from https://gisgeography.com/sentinel-2-bands-combinations/

Junpen A, Pansuk J, Kamnoet O, Cheewaphongphan P, Garivait S. (2018). Emission of Air Pollutants from Rice Residue Open Burning in Thailand. Atmosphere, 9(11) :449. https://doi.org/10.3390/atmos9110449

Keeley, J. E. (2009). Fire intensity, fire severity and burn severity: A brief review and suggested usage. International Journal of Wildland Fire, 18(1), 116–126.

Katagis, T., Gitas, I. Z. (2022). Assessing the Accuracy of MODIS MCD64A1 C6 and FireCCI51 Burned Area Products in Mediterranean Ecosystems. Remote Sensing. 14 (3).

Khamrueangwong, T., Kamthonkiat, D. (2021). Burn indices from Landsat 8 : Restrictions on Its Application. BURAPHA SCIENCE JOURNAL, 26(2), 1308-1325.

Kovacs, K.D. (2019). Evaluation of Burned Areas With Sentinel-2 Using Snap: The Case of Kineta and Mati, Greece, July 2018. Geographia Technica, 14 (2), 20-38. DOI: 10.21163/GT_2019.142.03

Linta, N., Mahavik, N., Chatsudarat, S., Seejata, K., & Yodying, A. (2021). Analysis of Burning Area from Forest Fire using Sentinel-2 image: A Case Study of Pai, Mae Hong Son Province. Journal of Applied Informatics and Technology, 3(2), 101–121. https://doi.org/10.14456/jait.2021.9

Mohammad, L., Bandyopadhyay, J., Sk, R., Mondal, I., Nguyen, T., Lama G., Anh D. (2023). Estimation of agricultural burned affected area using NDVI and dNBR satellite-based empirical models. Journal of Environmental Management. 343, 118226. https://doi.org/10.1016/j.jenvman.2023.118226

NASA. (2023). Harmonized Landsat and Sentinel-2. Retrieved from https://hls.gsfc.nasa.gov/

Praesriwarothai, U. (2021). Study of Active Fire Evolution in Northern Thailand Using Density Based Spatial Clustering of Applications with Noise (DBSCAN) and Kernel Density Estimation (KDE). Chulalongkorn University Theses and Dissertations (Chula ETD). https://digital.car.chula.ac.th/chulaetd/5520

Rongmuang, K. (2015). Assessment of pollutant emission from open field burning of agricultural. Degree of Master of Engineering in Agricultural and Food. Suranaree University of Technology.

Ruthamnong, S. (2019). Burned area extraction using multitemporal difference of spectral indices from Landsat 8 data: A case study of Khlong Wang Chao, Klong Lan and Mae Wong National Park. The Golden Teak : Humanity and Social Science Journal (GTHJ.) 25(2), 49-65.

Sentinel online. (n.d.). Level-2A Algorithm Overview. Retrieved from https://sentinels.copernicus.eu/web/sentinel/technical-guides/sentinel-2-msi/level-2a/algorithm-overview

Sentinelhub. (2021). Sentinel-2 processing baseline changes and harmonizeValues. Retrieved from https://forum.sentinel-hub.com/t/sentinel-2-processing-baseline-changes-and-harmonizevalues/4635

Sentinelhub2. (n.d.). NDWI Normalized Difference Water Index. Retrieved from https://custom-scripts.sentinel-hub.com/custom-scripts/sentinel-2/ndwi/

Kanjanarueng, Y, Miangbua, O and Ratanakaew, T. (2023). Cost-Benefit Analysis of Agricultural Waste Management Methods (Research Report). National Research Council of Thailand.